

Weierstraß-Institut
für Angewandte Analysis und Stochastik
Leibniz-Institut im Forschungsverbund Berlin e. V.

Preprint

ISSN 2198-5855

Doping optimization for optoelectronic devices

Dirk Peschka, Nella Rotundo, Marita Thomas

submitted: April 20, 2018

Weierstraß-Institut
Mohrenstr. 39
10117 Berlin
Germany
E-Mail: dirk.peschka@wias-berlin.de
nella.rotundo@wias-berlin.de
marita.thomas@wias-berlin.de

No. 2501
Berlin 2018



2010 *Mathematics Subject Classification.* 82D37, 49J20, 49M15.

Key words and phrases. Optoelectronics, drift-diffusion model, second-order optimization.

Financial support by DFG via project B4 in SFB 787 and by the Einstein Foundation Berlin via the MATHEON projects OT1/OT8 in ECMath. The authors thank P. Farrell, M. Liero, A. Glitzky and T. Koprucki for fruitful discussions.

Edited by
Weierstraß-Institut für Angewandte Analysis und Stochastik (WIAS)
Leibniz-Institut im Forschungsverbund Berlin e. V.
Mohrenstraße 39
10117 Berlin
Germany

Fax: +49 30 20372-303
E-Mail: preprint@wias-berlin.de
World Wide Web: <http://www.wias-berlin.de/>

Doping optimization for optoelectronic devices

Dirk Peschka, Nella Rotundo, Marita Thomas

Abstract

We present a mathematical and numerical framework for the optimal design of doping profiles for optoelectronic devices using methods from mathematical optimization. With the goal to maximize light emission and reduce the thresholds of an edge-emitting laser, we consider a drift-diffusion model for charge transport and include modal gain and total current into a cost functional, which we optimize in cross sections of the emitter. We present 1D and 2D results for exemplary setups that point out possible routes for device improvement.

1 Motivation and approach

Silicon photonics has a high potential for novel solutions in microelectronics, *e.g.*, for high-speed data transfer via optical on-chip communication or for bio-sensing. In this regard, the engineering of mechanical strains or of electronic doping provides feasible ways to enhance optoelectronic properties of semiconductor lasers in a desired direction. This is in particular important for germanium-based lasers, which aspire to serve as integrated light sources for silicon photonics. However, since germanium is an indirect band-gap material, low heat generation and low lasing threshold currents are crucial design properties. However, for most classical device designs this is certainly impossible to achieve without further optimization.

There have been several studies investigating the mathematical optimization of electronic transport in semiconductor devices using optimal control methods, *e.g.*, see [1] and [2]. We present an effort to extend these existing mathematical methods systematically to *optoelectronic* devices, specifically to germanium-based emitters. While the proof-of-concept for germanium-based emitters has been shown by [3], such devices still suffer from unpractically high lasing thresholds which result in device heating and quick degradation. In order to support the development of Ge-based CMOS-compatible emitter designs, we present a doping optimization approach below threshold with the attempt to raise the modal net-gain above the lasing threshold, while simultaneously controlling the electrical current.

It was shown that a combination of tensile strain and high n -doping transforms germanium into a suitable optically active medium for an edge-emitting laser, *cf.* [3] and [4]. Without any doubt a certain amount of mechanical strain is absolutely necessary in order to enhance light emission. However, beside its obvious impact on the Ohmic resistance of a device, doping can influence optical properties in various ways. For instance, in [5] it was shown that guiding the electron current through an aperture into the optically active region can be beneficial for lowering the laser threshold. Such a design can be realized through pocket doping, *e.g.* [6]. Furthermore, it has been observed that doping may have drastic impact on non-radiative recombination, *cf.* [7]. By indirectly tuning the carrier density, doping also affects stimulated emission and free carrier absorption. This determines the type of doping in optically active region.

Motivated by this potential and need for further improvement, we study the problem of finding an optimal doping profile $c : \Omega \subset \mathbb{R}^d \rightarrow \mathbb{R}$ for spatial dimensions $d \in \{1, 2\}$, aiming at enhanced laser

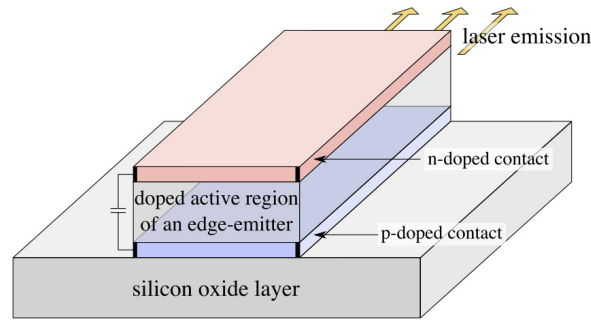
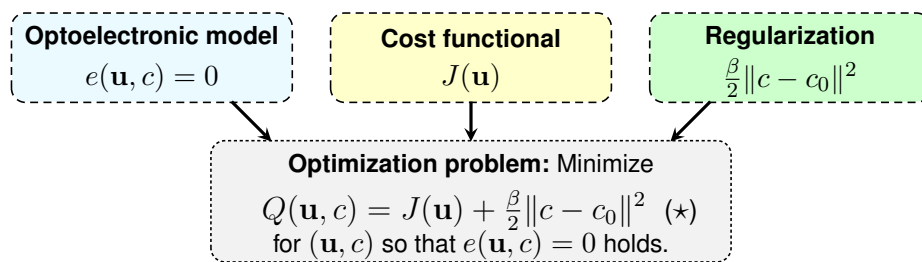


Figure 1: Sketch of a contacted edge-emitter, where the doping profile $c(x)$ in the optically active region is to be optimized.

light emission, cf. Fig. 1.

In order to properly set up the optoelectronic optimization problem we use the following main three ingredients: 1.) an *optoelectronic model*, 2.) a *cost functional*, and 3.) a *regularization of the cost functional*.



Here $e(\mathbf{u}, c) = 0$ is the partial differential equation (PDE) for charge transport in a semiconductor, and might contain models from optics such as a Helmholtz problem or rate equations for stimulated emission. With \mathbf{u} we denote solutions of this PDE system, here it will be the electrostatic and quasi-Fermi potentials, and $c(x)$ denotes the control/design parameter, here the doping. The purpose of the regularization $\frac{\beta}{2} \|c - c_0\|^2$ is to make the optimization problem well-posed, so that minimizers do exist. Furthermore, the regularization might include constraints on the design, *e.g.*, related to the manufacturability of the doping profile. Additionally, one can use the regularization to impose that the minimizer is close to an existing and manufacturable reference doping $c_0(x)$. In the cost functional J we encode our physically motivated optimization goals, *i.e.*, high modal gain and low electrical threshold current. In the following we will discuss how to set up such an optimization problem, including some practical hints in how certain parameter affect optimal dopings.

2 Optoelectronic model and doping optimization

We seek the electrostatic potential $\psi(t, x)$, the electron and hole quasi-Fermi potentials $\phi_n(t, x)$, $\phi_p(t, x)$, and the photon number $\gamma_k(t)$, such that

$$0 = -\nabla \cdot (\epsilon_r \nabla \psi) - (c + p - n), \quad (1a)$$

$$0 = \dot{n} - \nabla \cdot \mathbf{j}_n + R_{nr} + g(n, p, \psi) \gamma_k \Theta^2, \quad (1b)$$

$$0 = \dot{p} + \nabla \cdot \mathbf{j}_p + R_{nr} + g(n, p, \psi) \gamma_k \Theta^2, \quad (1c)$$

$$0 = \dot{\gamma}_k - \frac{\gamma_k}{|\Omega|} \int_{\Omega} (g - \ell) \Theta^2 dx, \quad (1d)$$

with charge fluxes $\mathbf{j}_n = -\mu_n n \nabla \phi_n$ and $\mathbf{j}_p = -\mu_p p \nabla \phi_p$, non-radiative recombination rates R_{nr} , gain g , and losses ℓ . The quasi-Fermi potentials ϕ_n, ϕ_p are implicitly defined by the general equation of state

$$n = N_c F\left(\frac{q(\psi - \phi_n) - E_c}{k_B T}\right) \quad \text{and} \quad p = N_v F\left(\frac{E_v - q(\psi - \phi_p)}{k_B T}\right). \quad (2)$$

Then, the standard drift-diffusion formulation is obtained by using Boltzmann statistics, *i.e.*, $F(s) = e^s$. The model (1) is motivated by [8], for which it was shown in [9] that it has a particular gradient structure. The model (1) is supplemented with Dirichlet conditions with external applied voltage V_{ext} at Ohmic contacts Γ_c and with homogeneous natural boundary conditions $\nu \cdot \mathbf{j}_n = \nu \cdot \mathbf{j}_p = \nu \cdot \nabla \psi = 0$ on the remaining boundary.

The non-radiative recombination rates in the model are of the standard form $R_{nr} = r(n, p)(np - n_i^2)$ and contain contributions from Shockley-Read-Hall and Auger recombination. The photon number $\gamma_k(t)$ in (1d) corresponds to an optical mode solving a scalar Helmholtz eigenvalue problem

$$[\Delta + k^2 \hat{\epsilon} - \kappa^2] \Theta = 0, \quad (3)$$

with wavenumber k and complex dielectric constant $\hat{\epsilon} = (n_r + \frac{i}{2k}g)^2$. Applying a perturbation argument on (3) determines the rates in (1). For the moment we perform optimization below threshold, so that it makes sense to neglect (1d) in $e(\mathbf{u}, c)$. Instead, we incorporate the modal gain into the cost functional J of the optimization. For brevity of our discussion, we will neglect non-radiative recombination R_{nr} and excluded further cavity losses and stimulated emission from the discussion. By setting time-derivatives $\dot{n} = \dot{p} = 0$ in (1a-c) we seek stationary solutions, defining the optoelectronic system $e(\mathbf{u}, c) = 0$. The resulting system of partial differential equations is called the stationary van-Roosbroeck system and its mathematical analysis can e.g. be found in [10].

In order to find an optimal doping c_{opt} , we write the solutions of (1a-c) in the compact vectorial form $\mathbf{u} = (\psi, \phi_n, \phi_p)$. We are interested in high modal gain J_g and low (threshold) currents J_c through contacts $\Gamma_c \subset \Gamma_D$, which results in the constrained optimization problem (\star) with cost functional $J(\mathbf{u})$ defined as

$$J = J_g + \alpha J_c, \quad J_c = \left(\int_{\Gamma_c} \nu \cdot \mathbf{j} da \right)^m, \quad J_g = \int_{\Omega} -(g - \ell) \Theta^2 dx, \quad (4)$$

where g and ℓ refer to optical gains and losses, $\mathbf{j} = \mathbf{j}_n + \mathbf{j}_p$ is the total current, and we use $m = 1, 2$. The interpretation of the scalar parameter $\alpha \geq 0$ is to balance the relative importance of our two physically motivated optimization goals of high modal gain and low electrical threshold currents, *i.e.*, for $\alpha = 0$ only the modal gain is maximized whereas for $\alpha > 0$ we trade some of the modal gain in order to decrease the total electrical current. Moreover, the role of the parameter β is to weight the

relative importance of the cost J and a mathematical regularization of the doping profile $c(x)$. For this regularization we use

$$\|c - c_0\|^2 = \int_{\Omega} (c - c_0)^2 + |\nabla(c - c_0)|^2 dx, \quad (5)$$

the H^1 -norm with the given reference doping $c_0(x)$. For H^1 -regularization, the doping at the boundary is not necessarily fixed, so that at Ohmic contacts the boundary value depends nonlinearly on the doping. When using an L^2 -regularization, one must not fix the doping at the boundary, which then renders Ohmic contacts useless. Further details on the mathematical analysis, in particular the choice of admissible dopings and regularizations, can be found in [1] and in [11].

Note that, in contrast to low-dimensional parametric optimization, (\star) represents an infinite-dimensional constrained optimization problem in function spaces, which after spatial discretization becomes a high-dimensional problem for which one desires to show mesh-independent convergence, *e.g.*, as considered in [12].

3 Numerics for optoelectronic model and optimization solver

The numerical solution of the stationary semiconductor charge transport equation (1a-c) relies on a P1 finite element method, *cf.* also [13]. We seek the electrostatic potential and the quasi-Fermi potentials $\mathbf{u} = (\psi, \phi_n, \phi_p)$, such that (1) can be written in a weak form $\langle e_{\psi}, w_1 \rangle + \langle e_n, w_2 \rangle + \langle e_p, w_3 \rangle = 0$ as

$$0 = \langle e_{\psi}(\mathbf{u}, c), w_1 \rangle = \int \epsilon_r \nabla \psi \cdot \nabla w_1 - (c + p - n)w_1 dx, \quad (6a)$$

$$0 = \langle e_n(\mathbf{u}, c), w_2 \rangle = \int \mu_n n \nabla \phi_n \cdot \nabla w_2 - R_{nr} w_2 dx, \quad (6b)$$

$$0 = \langle e_p(\mathbf{u}, c), w_3 \rangle = \int \mu_p p \nabla \phi_p \cdot \nabla w_3 + R_{nr} w_3 dx, \quad (6c)$$

for all test functions w_i . Using $\mathbf{e}(\mathbf{u}, c) = (e_{\psi}, e_n, e_p)$ and $\mathbf{w} = (w_1, w_2, w_3)$ the weak form is abbreviated $\langle \mathbf{e}(\mathbf{u}, c), \mathbf{w} \rangle = 0$ for all $\mathbf{w} \in H^1(\Omega)$. The densities n, p depend explicitly on \mathbf{u} via the equation of state (2). We solve (6) using a Newton scheme $\delta \mathbf{u} = \mathbf{u}_{k+1} - \mathbf{u}_k = -(\partial_{\mathbf{u}} \mathbf{e}(\mathbf{u}_k, c))^{-1} \mathbf{e}(\mathbf{u}_k, c)$. Dirichlet boundary conditions are imposed using Lagrange multipliers, which are omitted here for brevity.

To ensure convergence of the Newton method we first solve the equilibrium problem for $V_{\text{ext}} = 0$, which reduces to the nonlinear Poisson equation $e_{\psi}(\mathbf{u}_{\text{eq}}, c) = 0$ since $e_n = e_p = 0$ are automatically satisfied with $\phi_n = \phi_p = 0$. The Newton iteration for the nonlinear Poisson equation is initialized with $\mathbf{u}_0 = (\psi_0, 0, 0)$ so that local charge neutrality $c = (n - p)_{\mathbf{u}_0}$ automatically holds. Then, we gradually increase V_{ext} and solve (6) initializing with the previous solution until the desired V_{ext} is reached. Usually 3-5 Newton steps are necessary for Newton's method to reach numerical precision, whereas 10-100 uniform increments of V_{ext} are sufficient.

For the doping optimization we also use Newton's method applied to the the first-order optimality conditions of the constrained optimization problem (\star) , which, using the Lagrangian $\mathcal{L}(\mathbf{u}, c, \lambda) = Q(\mathbf{u}, c) + \langle \mathbf{e}(\mathbf{u}, c), \lambda \rangle$, can be written as

$$\mathcal{L}'(\mathbf{u}_{\text{opt}}, c_{\text{opt}}, \lambda_{\text{opt}}) = \begin{pmatrix} \langle \mathbf{e}_{\mathbf{u}}, \lambda_{\text{opt}} \rangle + Q_{\mathbf{u}} \\ \langle \mathbf{e}_c, \lambda_{\text{opt}} \rangle + Q_c \\ \mathbf{e} \end{pmatrix} \stackrel{!}{=} 0, \quad (7)$$

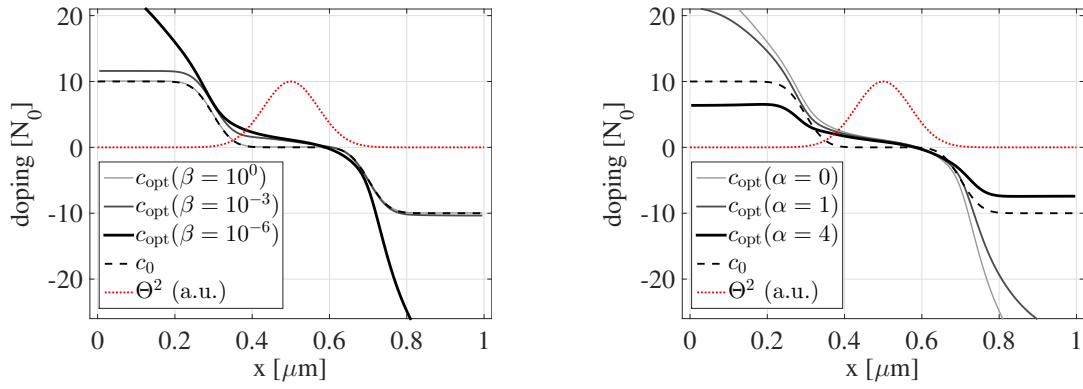


Figure 2: Optimal doping at $V_{\text{ext}} = 0.85 V$ showing the influence of using (left) 3 different β with $\alpha = 0$ or using (right) 3 different α with $\beta = 10^{-6}$.

where we can also write $\langle \mathbf{e}_{\mathbf{u}}, \lambda \rangle = \mathbf{e}_{\mathbf{u}}^* \lambda$ or $\langle \mathbf{e}_c, \lambda \rangle = \mathbf{e}_c^* \lambda$, the star denotes the adjoint, and subscript indices \mathbf{u}, c refer to derivatives. The bracket construction has to be understood in the sense $\langle \mathbf{e}, \lambda \rangle = \langle e_\psi, \lambda_1 \rangle + \langle e_n, \lambda_2 \rangle + \langle e_p, \lambda_3 \rangle$ with components as defined in (6). Using second-derivatives of \mathcal{L} and the structure of Q we construct the Newton method, which explicitly reads

$$\mathcal{L}'' \begin{pmatrix} \delta \mathbf{u} \\ \delta c \\ \delta \lambda \end{pmatrix} = \begin{pmatrix} Q_{\mathbf{u}\mathbf{u}} + \langle \mathbf{e}_{\mathbf{u}\mathbf{u}}, \lambda \rangle & 0 & \mathbf{e}_{\mathbf{u}}^* \\ 0 & Q_{cc} + \langle \mathbf{e}_{cc}, \lambda \rangle & \mathbf{e}_c^* \\ \mathbf{e}_{\mathbf{u}} & \mathbf{e}_c & 0 \end{pmatrix} \begin{pmatrix} \delta \mathbf{u} \\ \delta c \\ \delta \lambda \end{pmatrix} = - \begin{pmatrix} 0 \\ \mathbf{e}_c^* \lambda + Q_c \\ 0 \end{pmatrix}, \quad (8)$$

using that $\mathbf{e} = 0$ and the adjoint equation $\mathbf{e}_{\mathbf{u}}^* \lambda = -Q_{\mathbf{u}}$ are satisfied. Here we can eliminate $\delta \mathbf{u} = -\mathbf{e}_{\mathbf{u}}^{-1} \mathbf{e}_c \delta c$ and $\delta \lambda = -(\mathbf{e}_{\mathbf{u}}^{-1})^* (Q_{\mathbf{u}\mathbf{u}} + \langle \mathbf{e}_{\mathbf{u}\mathbf{u}}, \lambda \rangle) \delta \mathbf{u} \hat{\mathbf{A}} \hat{\mathbf{a}}$ to finally get

$$H \delta c = [Q_{cc} + \langle \mathbf{e}_{cc}, \lambda \rangle + \mathbf{e}_c^* (\mathbf{e}_{\mathbf{u}}^{-1})^* (Q_{\mathbf{u}\mathbf{u}} + \langle \mathbf{e}_{\mathbf{u}\mathbf{u}}, \lambda \rangle) \mathbf{e}_{\mathbf{u}}^{-1} \mathbf{e}_c] \delta c = -\mathbf{e}_c^* \lambda - Q_c. \quad (9)$$

Our approach is to first discretize Q , \mathbf{e} and then compute all needed derivatives with respect to c , \mathbf{u} . Such an approach to device optimization is advantageous due to its fast convergence, which typically does not depend on the discretization. However, since H involves the inverse of $\mathbf{e}_{\mathbf{u}}$ and \mathbf{e}_c^* , it cannot be constructed explicitly. Instead, we can define its action on an arbitrary vector and compute $\delta c = c_{k+1} - c_k$ using an inner CG iteration inside each Newton step.

4 Discussion of optimized doping profiles

Here we present some results obtained for dimensions $d = 1$ and $d = 2$. The used gain model is motivated in [5] and in [11], the numerical values are representative for strained germanium but are not tuned towards quantitative predictions. For material parameters we use $N_c = 10^{19} \text{ cm}^{-3}$, $N_v = 4 \cdot 10^{18} \text{ cm}^{-3}$ and a bandgap $E_g = 0.7 \text{ eV}$ representative for bulk germanium at $T = 300 \text{ K}$. In the following we discuss mathematical and physical aspects of the optimization framework in the context of optoelectronics. Note, for $d = 1$ we use $m = 2$, whereas for $d = 2$ we use $m = 1$ in J_c .

For $d = 1$ we optimize in $\Omega = [0, 1] \mu\text{m}$ using a smooth pin-type reference doping c_0 , which is of the order $N_0 = 10^{19} \text{ cm}^{-3}$. The considered range of bias values is $V_{\text{ext}} = 0.65 - 0.85 \text{ V}$ and can be used to select the total current J_c of the device. In general the lasing threshold is near $V_{\text{ext}} \approx e^{-1} (E_g + \hbar\omega)$, which for our parameter setup is expect to be slightly above $e^{-1} E_g$. This is why we show representative optimized dopings at $V_{\text{ext}} = 0.85 \text{ V}$ for different α and β in Fig. 2. In general, the shape of c_{opt} in Fig. 2

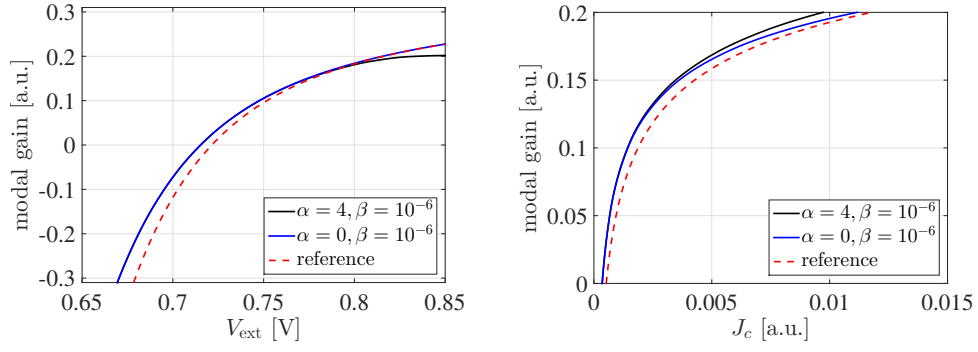


Figure 3: modal gain J_g for $d = 1$ (left) as a function of bias V_{ext} and (right) as a function of the corresponding total current $J_c(V_{\text{ext}})$ for the reference doping c_0 and for the optimized doping c_{opt} for different α

suggest a low doping where the optical mode is located is higher doping outside the support of the mode Θ^2 . Interestingly, the slight asymmetry in the free carrier absorption $f_p = 5f_n$ in the gain model

$$g(\mathbf{u}) = \kappa \left(e^{\frac{-\hbar\omega}{k_B T}} - e^{\frac{-qU_F}{k_B T}} \right) \left(\frac{np}{N_0^2} \right)^\gamma, \quad \ell(\mathbf{u}) = f_n n + f_p p, \quad (10)$$

with $qU_F = k_B T (F^{-1}(n/N_c) + F^{-1}(p/N_v)) + E_g$ leads to an asymmetric doping profile favoring n doping in the active region.

For $\beta \sim 1$ the optimal doping is close to the reference doping c_0 , whereas for $\beta \rightarrow 0$ the doping will be optimized so that the modal gain J_g is maximized. Since the optical mode Θ^2 is only supported in the interval $0.3\mu m < x < 0.7\mu m$, visible in the dashed red line in Fig. 2, the doping outside this region is not affected by J_g and therefore still depends on the regularization, as we previously discussed in [11]. This effect is clearly visible in the extremely high doping for $\beta = 10^{-6}$ in the left panel of Fig. 2. However, carefully selecting $\alpha > 0$ we can enforce lower electrical currents at the expense of slightly lower gains. For instance, in the right panel of Fig. 2 with $\alpha = 4$ and $\beta = 10^{-6}$ does not strongly impact the doping in the region $0.3\mu m < x < 0.7\mu m$, whereas outside this region lower dopings are needed in order to achieve lower currents. In addition to the parameters α, β which appear in the definition of the cost functional, also the external bias V_{ext} is a parameter the optimal doping depends on. Therefore, in Fig. 3 we show what modal gain J_g can be achieved for exemplary values $\alpha = 0$ and $\alpha = 4$ and $\beta = 10^{-6}$ as a function of the bias V_{ext} in the left panel or plotted as a function of the corresponding current J_c in the right panel. We show the corresponding functionals evaluated for the reference doping as a comparison.

The simulations for $d = 2$ are shown in Fig. 4, except for the bias $V_{\text{ext}} = 0.7V$ the physical parameters are the same. The domain is a cavity that is cut into half at $x = 0.5\mu m$ with the corresponding optical mode $\Theta \sim \sin(\pi x[\mu m]) \sin(4\pi y[\mu m])$. The two contacts are at $x = 0$ with $y \leq 0$ and $y \geq 0.25\mu m$. Near the top and bottom, *i.e.*, for all x with $y \leq 0$ or $y \geq 0.25\mu m$, the doping is fixed, in all other places the doping is optimized. The results in Fig. 4 are computed on a rather coarse tensor-mesh with 2820 vertices and 8652 unknowns. Similar as for $d = 1$, the optimal doping c_{opt} is rather smooth where the optical mode is supported and its sign is determined by the free carrier absorption f_n, f_p . Outside this region the doping depends on the regularization, which is why again we study the limit $\beta \rightarrow 0$ and set $\beta = 10^{-4}$. Already for $\alpha = 0$, the middle panel of Fig. 4 shows that c_{opt} takes values with opposite sign counteracting the the doping near the contacts, which seems beneficial for the modal gain. As a side effect, the middle panel of Fig. 5 shows that the current for $\alpha = 0$ is also focussed towards the center of the optical mode. This is an improvement compared to

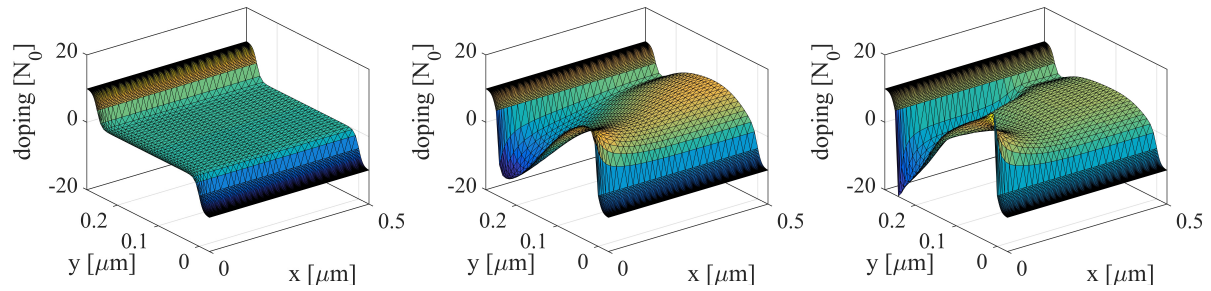


Figure 4: Doping for $\Omega = [0, 0.5]\mu m \times [-0.025, 0.275]\mu m$ showing (left) reference c_0 and (middle and right) optimal c_{opt} for $\beta = 10^{-4}$ with $\alpha = 0$ and $\alpha = 1/4$ respectively for $V_{\text{ext}} = 0.7V$.

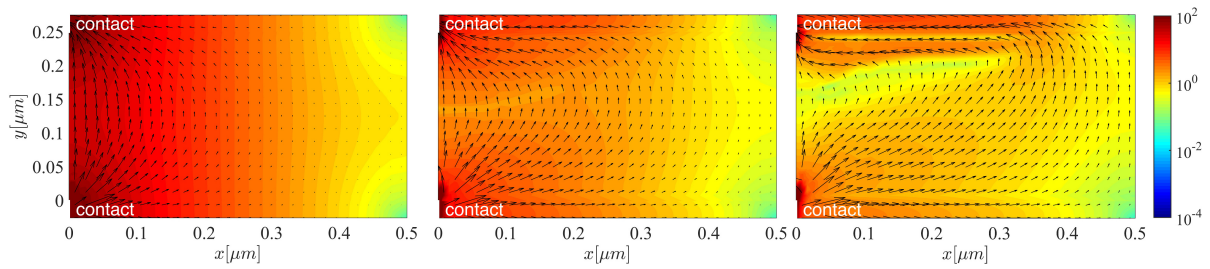


Figure 5: total current density (shading) and vector field (arrows) at $V_{\text{ext}} = 0.7V$ with logarithmic scaling (left) for the reference doping c_0 (middle) for c_{opt} and $\alpha = 0, \beta = 10^{-4}$ and (right) $\alpha = 1/4, \beta = 10^{-4}$ corresponding to the dopings in Fig. 4

the shortcut current visible for the reference doping in the left panel of Fig. 5. Solving the optimization problem with $\alpha = 1/4$ even improves this focussing by creating sharper doping pockets visible in the right panel of Fig. 4, which appears as if the current would be guided through an aperture created by the doping in the right panel of Fig. 5.

5 Conclusion

Compared to low-dimensional parameter studies, infinite-dimensional doping optimization provides a systematic method to gain insight into the achievable optoelectronic performance. When designing such a toolbox, much implementation effort goes into computation higher-order derivatives of the model. However, this requires direct control over the solver implementation. From a modeling point-of-view, achieving reasonable optimal designs also requires a good understanding of the mathematical parameters involved in the optimization. Further improvements are viable by model improvement and validation.

References

- [1] Michael Hinze and René Pinnau. An optimal control approach to semiconductor design. *Mathematical Models and Methods in Applied Sciences*, 12(01):89–107, 2002.
- [2] Martin Burger and René Pinnau. Fast optimal design of semiconductor devices. *SIAM Journal on Applied Mathematics*, 64(1):108–126, 2003.

- [3] Jifeng Liu, Xiaochen Sun, Rodolfo Camacho-Aguilera, Lionel C Kimerling, and Jurgen Michel. Ge-on-Si laser operating at room temperature. *Optics letters*, 35(5):679–681, 2010.
- [4] Birendra Dutt, Devanand S Sukhdeo, Donguk Nam, Boris M Vulovic, Ze Yuan, and Krishna C Saraswat. Roadmap to an efficient germanium-on-silicon laser: strain vs. n-type doping. *IEEE Photonics Journal*, 4(5):2002–2009, 2012.
- [5] Dirk Peschka, Marita Thomas, Annegret Glitzky, Reiner Nürnberg, Klaus Gärtner, Michele Virgilio, Subhajit Guha, Thomas Schroeder, Giovanni Capellini, and Thomas Koprucki. Modeling of edge-emitting lasers based on tensile strained germanium microstrips. *IEEE Photonics*, 7, 2015.
- [6] Venkatagirish Nagavarapu, Ritesh Jhaveri, and Jason CS Woo. The tunnel source (pnpn) n-mosfet: A novel high performance transistor. *IEEE Transactions on Electron Devices*, 55(4):1013–1019, 2008.
- [7] Michael R Barget, Michele Virgilio, Giovanni Capellini, Yuji Yamamoto, and Thomas Schroeder. The impact of donors on recombination mechanisms in heavily doped Ge/Si layers. *Journal of Applied Physics*, 121(24):245701, 2017.
- [8] Uwe Bandelow, Herbert Gajewski, and Rolf Hünlich. *Fabry-Perot Lasers: Thermodynamics-Based Modeling*, pages 63–85. Springer New York, 2005.
- [9] Alexander Mielke, Dirk Peschka, Nella Rotundo, and Marita Thomas. Gradient structures for optoelectronic models of semiconductors. In *Matheon preprint (to appear in Proceedings of ECMI 2016)*, 2016.
- [10] Peter A Markowich. *The stationary semiconductor device equations*. Springer Science & Business Media, 1986.
- [11] Dirk Peschka, Nella Rotundo, and Marita Thomas. Towards doping optimization of semiconductor lasers. *Journal of Computational and Theoretical Transport*, 45(5):410–423, 2016.
- [12] Martin Weiser, Anton Schiela, and Peter Deufhard. Asymptotic mesh independence of Newton’s method revisited. *SIAM Journal on Numerical Analysis*, 42(5):1830–1845, 2005.
- [13] M Auf der Maur. *A multiscale simulation environment for electronic and optoelectronic devices*. PhD thesis, University of Rome Tor Vergata, 2008.